

PHOTODEGRADATION OF LIQUID WASTE USING ZnO/GRAPHENE-LIKE COMPOSITES

Desi Heltina*, Raihan Daffansyah Sinaga*, Yayan Setiawan*, M Iwan Fermi*, Amun Amri*

*Department of Chemical Engineering, Faculty of Engineering, Pekanbaru, Indonesia,
desi.heltina@lecturer.unri.ac.id, raihan.daffansyah@gmail.com, setiayan26@gmail.com,
miwanf@eng.unri.ac.id, amun.amri@eng.unri.ac.id

Email Correspondence : desi.heltina@lecturer.unri.ac.id

Received : December 6, 2023

Accepted : June 12, 2024

Published : June 30, 2024

Abstract: The development of industries such as textiles, dyes, plastics, medicines, cosmetics, and others is increasing along with a rise in production, leading to a high amount of liquid waste generated. Non-biodegradable, toxic, and carcinogenic liquid waste can cause environmental pollution to surrounding water. To address this challenge, biomass waste such as palm kernel shells can be used to treat liquid waste by compositing it with photocatalyst materials. Therefore, this research aimed to obtain ZnO/graphene-like composites to degrade liquid waste. ZnO/Graphene-like composites were synthesized using the solvothermal method, followed by calcination. The performance test was carried out by varying the types of methylene blue, methyl orange, and phenol waste with an initial concentration of 10 ppm, alongside the variations of ultraviolet (UV) and mercury lamps. Subsequently, characterization was carried out using SEM, XRD, FTIR, BET, UV-Vis DRS, and UV-Vis Spectrophotometer. The results showed that the percent degradation of methylene blue under UV and mercury were 83.42% and 84.93 % respectively, while methyl orange in the same conditions was 94.83% and 97.17%, respectively. Furthermore, the percent degradation of phenol in UV light and mercury were 86.03% and 89.62%, respectively. This showed that the use of mercury lamps on methyl orange was more effective than UV lamps on methylene blue and phenol.

Keywords: Photodegradation; Photocatalytic; Graphene-like; liquid waste; ZnO

Abstrak: Perkembangan industri seperti industri tekstil, pewarna, plastik, obat-obatan, kosmetik, dan lain-lain semakin meningkat dengan seiring bertambahnya jumlah produksi sehingga jumlah limbah yang dihasilkan juga meningkat salah satunya limbah cair. Limbah cair yang tidak dapat terurai secara biologis, beracun, dan karsinogenik ke perairan terdekat mengakibatkan pencemaran lingkungan. Disisi lain, limbah biomassa seperti cangkang sawit dapat dimanfaatkan untuk mengolah limbah cair, salah satunya mengkompositkan dengan material fotokatalis. Penelitian ini bertujuan memperoleh komposit ZnO/graphene-like untuk mendegradasi limbah cair. Komposit ZnO/Graphene-like disintesis dengan metode solvothermal dan dikalsinasi. Uji kinerja komposit ZnO/graphene-like dilakukan dengan bervariasi jenis limbah *methylene blue*, *methyl orange* dan fenol dengan konsentrasi awal masing-masing 10 ppm serta dengan variasi lampu UV dan lampu merkuri. Komposit ZnO/Graphene-like dikarakterisasi menggunakan SEM, XRD, FTIR, BET, UV-Vis DRS dan UV-Vis Spektrofotometer. Hasil penelitian menunjukkan bahwa persen degradasi *methylene blue* di bawah sinar UV dan merkuri masing-masing sebesar 83,42% dan 84,93%, sedangkan *methyl orange* dengan sinar UV dan merkuri masing-masing sebesar 94,83% dan 97,17%. Selanjutnya, persen degradasi fenol dengan sinar UV dan merkuri masing-masing adalah

86,03% dan 89,62%. Hal ini menunjukkan bahwa penggunaan lampu merkuri pada *methyl orange* lebih efektif dibandingkan lampu UV pada *methylene blue* dan fenol.

Kata kunci: Fotodegradasi; Fotokatalis; *Graphene-like*; Limbah cair; ZnO

Recommended APA Citation :

Heltina, D., Sinaga, R. D., Setiawan, Y., Fermi, M. I., & Amri, A. (2024).
Photodegradation of Liquid Waste Using ZnO/Graphene-Like Composites.
Elkawnie, 10(1), 125-142. <https://doi.org/10.22373/ekw.v10i1.21000>

Introduction

Environmental pollution is a crucial issue with detrimental effects on human life. A significant portion of the problem is generated by industries such as the textile industry, dye manufacturing, plastics, pharmaceuticals, and cosmetics. This phenomenon causes harmful consequences for human health and aquatic biota through the release of non-biodegradable, toxic, and carcinogenic dyes into surrounding water (Yi et al., 2019).

Industrial activities in Indonesia have been experiencing rapid growth annually, as supported by data from the Ministry of Industry (*Kementerian Perindustrian*) through the National Industrial Information System (SIINas or *Sistem Informasi Industri Nasional*). In December 2022, there were 37,609 companies (per factory or business location), showing an approximately 23% increase from last year, and 188 industrial estate companies, or 21.3%, predominantly dominated by the garment industries (*Kementerian Perindustrian*, 2022).

The rapid increase in industrial production significantly correlates with the high amount of waste generated, particularly liquid waste. In industries, liquid waste generated often contains aromatics, hydrocarbons, halogens, and metals, posing a risk of severe impact when not treated properly. Furthermore, it contains organic and inorganic compounds with high concentrations in almost every process unit, leading to a reduction in water quality (Suchaya et al., 2016).

Liquid waste such as methylene blue, methyl orange, and phenol generated through industrial activities contain many harmful compounds that can cause cyanosis, tissue necrosis, vomiting, jaundice, shock, and increased heart rate (R. Ahmad & Kumar, 2010). These compounds contain azo dyes, which have a chromophore group -N=N- in molecular structure and are nonbiodegradable, and highly toxic with color pigments harmful to living things (Rafiq et al., 2021). Azo dyes are capable of causing cancer in humans and become more harmful when reduced to intermediate products under anaerobic conditions. (Kant, 2012) reported that among 70% of chemical compounds from textile dyes, 30% can cause incurable diseases. Moreover, approximately 40% of dyes used globally contain organically bound chlorine, which is widely recognized as a carcinogen.

Industrial wastewater often contains organic and inorganic contaminants that are detrimental to the environment (Pham et al., 2018). It also contains dyes

with several characteristics, such as large effluent volume, high chromaticity, elevated organic matter concentration, difficulty in biodegradation, and blockage of sunlight, reducing photosynthetic activity in the water. Additionally, low concentrations of dyes (<1 mg/L) can disturb the aquatic balance (Vandevivere et al., 1998).

According to (Kementerian Lingkungan Hidup, 1995) on the quality standards of liquid waste for industrial activities, dyes and phenol are allowed to be discharged into the environment at a maximum of 10 mg/L and 1 mg/L, respectively. Regarding management, several methods can be used to remove dyes and phenolic compounds in wastewater. These methods include adsorption, biodegradation, and chemicals such as chlorination and ozonation, which are effective in dealing with waste but require huge operational costs. Other commonly used methods include combined coagulation, electrochemical oxidation, flocculation, reverse osmosis, and adsorption using activated carbon. However, there are several disadvantages associated with the methods, such as the generation of new phases containing more concentrated pollutants (Wijaya et al., 2006). An alternative strategy that has been proven effective in treating liquid waste is the photocatalysis process due to its capacity to produce environmentally friendly compounds, namely CO₂ and H₂O (Safni et al., 2019).

The photocatalysis process is among the most developed methods of the Advanced Oxidation Process (AOP) in the degradation of organic pollutants. Currently, AOP has become an effective method for degrading organic pollutants (Behzadi et al., 2020) due to its low cost and high efficiency (Behzadi et al., 2020; Jarariya, 2022). Some water treatments based on AOP include the catalytic ozonation process (Wang et al., 2019), nanomaterial process (Bethi et al., 2016), RO membrane adsorption and filtration process (Wang et al., 2019); ozone, H₂O₂, sulfate process (Ike et al., 2019), sonolytic ozonation process (Merouani & Hamdaoui, 2019), O₂/H₂O₂, O₃/UV, O₃/electrocoagulation, and nanocatalyst ozonation process (Malik et al., 2020). This system combines the role of semiconductor catalysts and light as a photon source. When the catalyst is irradiated with photon energy equal to or greater than the catalyst band gap, electrons from the catalyst will be excited from the valence to the conduction band. This process produces electrons and holes, which react with hydroxyl groups from water molecules to form hydroxyl radicals. Moreover, these hydroxyl radicals act as a strong oxidizer for the degradation of compounds including methylene blue, methyl orange, and phenol. The expected end products of the process are simpler and more environmentally friendly compounds, namely CO₂ and H₂O (Safni et al., 2019).

Heterogeneous photocatalysis is a promising method capable of addressing environmental pollution due to the ability to oxidize organic matter thoroughly (Chiou et al., 2008). Light absorption range is an important factor that directly affects the photocatalytic activity of semiconductors (Enesca & Isac, 2020). This is because most substances absorb radiation in the ultraviolet (UV) or visible light

region and experience photodegradation in liquid media or solid conditions after exposure. Moreover, the rate of photochemical reactions depends on the intensity and wavelength of light, showing the need for careful regulation (I. Ahmad et al., 2006). Considering these factors, it is essential to identify semiconductor materials with optimal light absorption properties.

ZnO is a semiconductor material with a band gap width of 3.37 eV, and an excitation energy of 60 meV, capable of absorbing UV at room temperature (Choi et al., 2012). The high quantum efficiency, wide band gap, and non-toxic nature of ZnO facilitate extensive application in the photocatalytic degradation of organic pollutants. In comparison with TiO₂, it shows higher absorption efficiency in most of the solar/light spectrum (Ong et al., 2018). When ZnO is irradiated, a pair of positive holes and electrons are generated in the valence and conduction band. The reaction of the two positive holes and electrons produces OH radicals, which are oxidizing agents affecting the reaction with organic pollutants and causing degradation (Adeel et al., 2021).

In line with the advancement in semiconductor material, the exploitation of biomass has increased significantly as the most widespread form of renewable energy. This phenomenon has raised concerns regarding the impact of fossil fuel consumption, namely climate change, global warming, and its adverse effects on the environment. Biomass is generated from agricultural, animal, municipal solid waste, and industrial residues (Tursi, 2019). A significant product derived from biomass is biochar, a carbon-rich solid material that can be synthesized from lignocellulosic biomass, agricultural waste, manure, and other sources. The quality of biochar is determined by the fixed carbon content and the composition is very essential to determine the application (Weber & Quicker, 2018). Lignin and cellulose are considered the main constituents of biomass affecting the composition and properties of pyrolysis products (Tripathi et al., 2016). Charcoal generated from cellulose and hemicellulose components in biomass produces volatile products and lignin (Qu et al., 2011). Although cellulose and lignin contents can enhance biochar formation, the production is higher in biomass with more lignin compared to cellulose (Tripathi et al., 2016).

Oil palm shell is a type of lignocellulosic biomass, mainly consisting of cellulose, hemicellulose, and lignin (Abnisa et al., 2011). The content of palm kernel shell components includes 20.8% cellulose, 22.7% hemicellulose, and 50.7% lignin (Hamzah et al., 2019). Biomass containing more lignin has been shown to produce more charcoal (Antal & Grønli, 2003; Mok et al., 1992), while high cellulose and hemicellulose content support the production of liquid and gaseous products. (Kang et al., 2012) explored hydrothermal conversion with varying lignin and cellulose ratios, reporting that char yield increased, alongside a decrease in water and gas products with high lignin content.

(Chen et al., 2019) found that 14% ZnO/biochar composites were superior to pure ZnO in the photocatalytic degradation of methylene blue. According to (He

et al., 2021), the ZnO/biochar composite produced a high methylene blue degradation efficiency of 98% after 100 minutes. ZnO/biochar from peanut shells produced through the solvothermal-calcination method was also more efficient than pure ZnO (Yu et al., 2023). Although biochar has made progress in the modification of ZnO materials, the material still faces insufficient performance improvement due to the limited coverage area of the light source from the UV region to the visible (Vis) region.

Palm kernel shells can be used as a substitute material for graphene due to the presence of cellulose carbon, consisting of carbon-carbon. Therefore, this research aimed to synthesize biochar-based ZnO-Graphene-like composite material from palm kernel shells. The analysis was carried out to determine the optimum efficiency in degrading methylene blue, methyl orange, and phenol compounds in variations of UV light sources and mercury using ZnO/Graphene-like composites from palm kernel shells.

Method

Palm kernel shell biomass waste was washed using distilled water to remove impurities and dried at 120°C for 12 hours using an oven. After achieving a constant weight, the palm kernel shell was pulverized using a blender and crushed with a mortar. Subsequently, the resulting powder was sieved to obtain a fine form with a size of 100 mesh.

The ZnO/graphene-like synthesis process was carried out using solvothermal and calcination methods. A total of 5.484 g of $\text{Zn}(\text{NO}_3)_2 \cdot 6\text{H}_2\text{O}$ and 3 ml of glacial acetic acid were dissolved in 60 ml of ethanol. This was followed by the addition of 1.645 g of palm kernel shell, which was stirred and moved to the autoclave to be heated for 12 hours at 180°C. After the solvothermal process, centrifugation was carried out to separate the solids from the mixture and dried using an oven. The solid was calcined for 2 hours at 700°C using nitrogen gas with a temperature increase of 5°C/minute to form a composite (Yu et al., 2023).

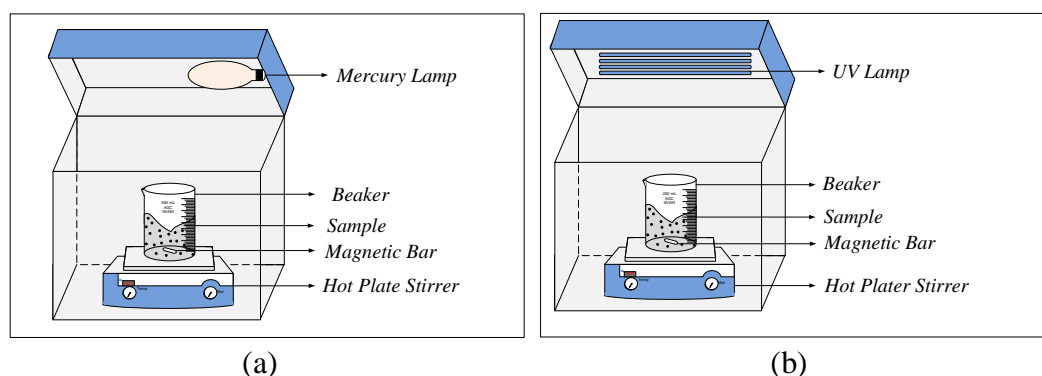


Figure 1. Schematic layout of Photoreactor apparatus (a) Mercury lamp (b) UV lamp

ZnO/Graphene-like composites obtained were tested for performance in degrading liquid waste compounds with a photocatalyst process. Initially, 0.3 g of composite was put into 300 mL of methylene blue solution with a concentration of 10 ppm and the mixture was stirred at 300 rpm at 30°C. Photocatalyst performance tests were carried out for 3.5 hours with the first 30 minutes under light-off and 2.5 hours at light-on conditions. Photodegradation of liquid waste was carried out in a photoreactor, as shown in Figure 1, with a variety of lamps, namely mercury (BOSSECOM 250W, 31,000 lux) and UV 10W 5 pieces (Sangkyo Denki CO., LTD Black Light Blue Lamp, 500 lux). The photoreactor used had dimensions of 50 x 40 x 60 cm with a sample and lamp distance of 20 cm. The same procedure was performed to degrade methyl orange and phenol. Subsequently, ZnO/Graphene-like composites were characterized using X-ray diffraction (XRD), Fourier Transform Infra-Red (FTIR), Scanning Electron Microscope (SEM), Brunauer Emmett Teller (BET), UV-DRS Spectrophotometer and UV-Vis Spectrophotometer.

Result

The ZnO/Graphene-like composite formed was analyzed using SEM characterization, as shown in Figure 2. Figure 2(a) shows the distributed ZnO covering the graphene-like. The distributed ZnO particles are sphere-shell/spherical, this follows the research conducted by (Yu et al., 2023) shown in Figure 2(b). The synthesized ZnO/Graphene-like composite material consists of 84.5% carbon atoms, 12% oxygen atoms, and 3.35% zinc atoms.

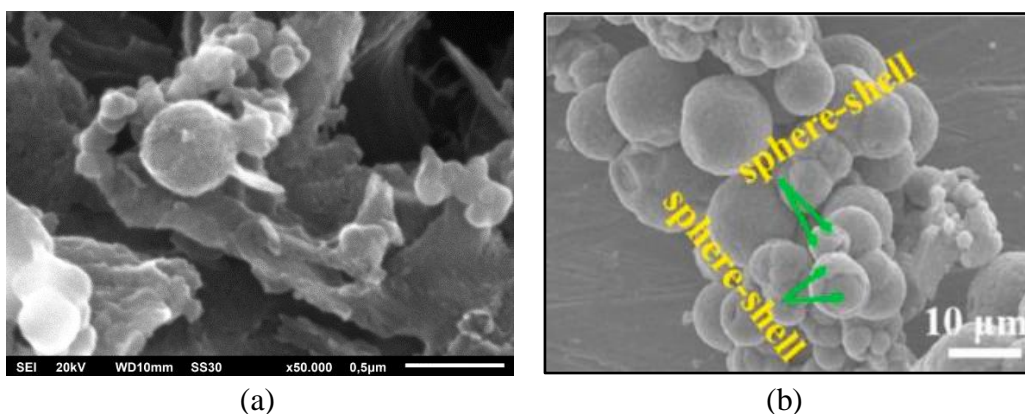


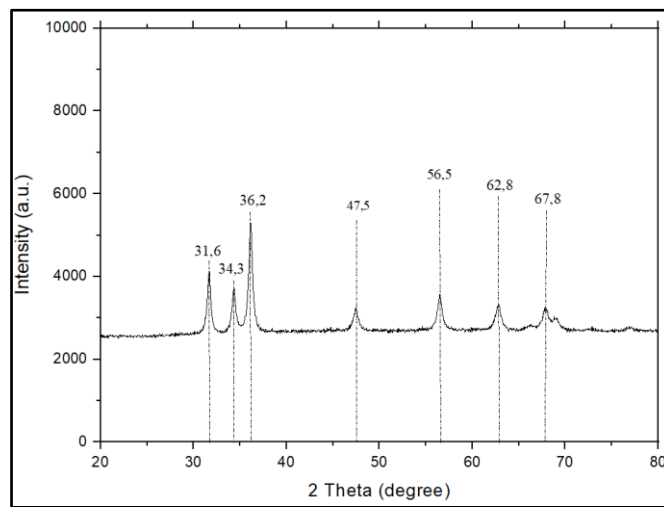
Figure 2. (a) SEM of ZnO/Graphene-like composites from palm kernel shell (b) SEM of ZnO/Graphene-like Biochar Peanut Shell (Yu et al., 2023)

Based on the results of XRD analysis, Figure 3 (a) showed that peaks at $2\theta = 31.6; 34.3; 36.2; 47.5; 56.5; 62.8; \text{ and } 67.8^\circ$ corresponded to (1 0 0), (1 0 1), (1 0 2), (1 1 0), (1 0 3), and (1 1 2) crystal planes, respectively, forming hexagonal wurtzite ZnO. This showed that ZnO/graphene-like biochar composites formed ZnO wurtzite crystals. To determine the average size of crystals, the Debye-Scherrer equation can be used (Sayem et al., 2024) :

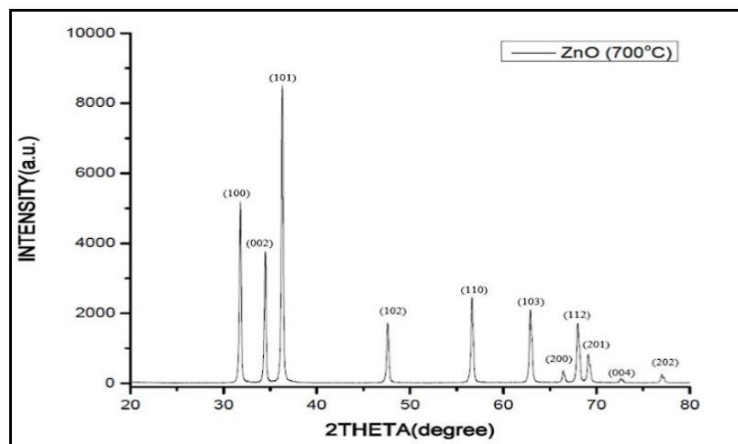
$$D=K \times \frac{\lambda}{\beta \cos \theta} \dots\dots\dots (1)$$

Where: D = average crystal size (nm), K = Scherrer constant (0.89), λ = wavelength of light used (Cu, λ = 0.15406 nm), β = full width at half maximum (FWHM), θ = diffraction angle

Based on the calculation results, the average crystal size of the 700°C ZnO/Graphene-like palm kernel shell biochar composite (Appendix B) is 26.0138 nm. Figure 3 (b) shows the XRD results of the synthesized nanoparticles and the standard ZnO, where the average size of crystallites with the precursor ($Zn(NO_3)_2 \cdot 6H_2O$) was approximately 18 nm (Parashar & Shukla, 2020). (Barzinjy & Azeez, 2020) stated that the size enlargement of ZnO is due to the agglomeration process of smaller particles.



(a)



(b)

Figure 3. (a) XRD of ZnO/Graphene-like Composites (b) XRD of pure ZnO (Parashar & Shukla, 2020)

In graphene-based materials, the oxidation state and the presence of oxidized species are known using FTIR infrared spectrum characterization.

Moreover, FTIR characterization analysis can provide information about interactions with other species based on the analysis of reactive peaks on the surface of the material. Figure 4 shows the results of FTIR analysis of ZnO/graphene-like composites.

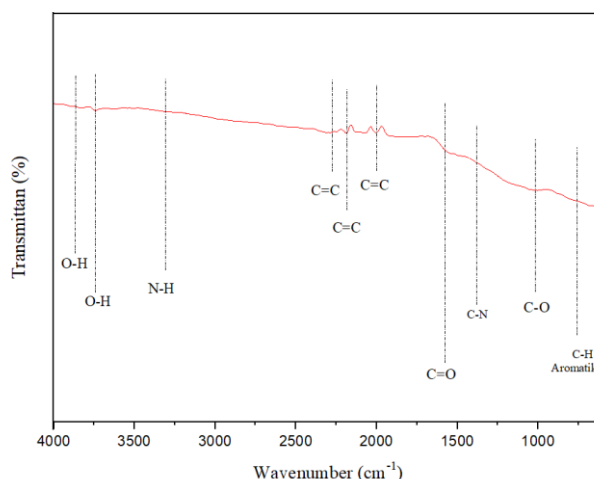


Figure 4. FTIR Characterization Analysis of ZnO/Graphene-like composites

Figure 4 shows that the presence of phenolic groups is confirmed in the wave number range between 3700-3900 cm^{-1} , indicating -OH groups (Tay-Agbozo et al., 2018). The O/N-H peak was identified at around 3420 cm^{-1} (Yu et al., 2023). At a wavelength of 2500-2000 cm^{-1} , the C=C group was identified (Mecozzi & Sturchio, 2017). Peaks at a wavelength around 1720 cm^{-1} showed C=O groups (Sudhakar et al., 2017). The epoxy and hydroxyl groups were significantly reduced due to deoxygenation, while the main peak (C-N strain) was detected between 1430 cm^{-1} to 1480 cm^{-1} (Sudhakar et al., 2017). C-O/N-C peak in the range of 1200-890 cm^{-1} became banded and shifted to higher wave numbers due to the conversion of $\text{sp}^3\text{-C-O/N-}$ to $\text{sp}^2\text{-C-O/N-}$ at high temperatures (Yu et al., 2023). The peak at wavelengths 860-680 cm^{-1} identified the stretching vibration of the C-H Aromatic bond (Jin et al., 2022). OH, C=C, C-N, and C-O groups identified in FTIR analysis showed the functional groups found in N-Graphene (Sudhakar et al., 2017). Composites containing alkyl, aromatic, and oxygen-containing groups could modify the structure of biochar to provide several potential active sites as well as improve the adsorption and degradation properties (Duan et al., 2015).

The surface area of photocatalyst material is an essential parameter that affects the photocatalysis process, determining the adsorption capacity of organic pollutants. It also makes more contact between pollutants and the catalyst, thereby influencing the photocatalytic process, particularly the degradation time (Farghali et al., 2016). Table 1 shows the comparison of surface area for pure ZnO and ZnO/Graphene-like, indicating that the addition of graphene-like increases the surface area of the ZnO photocatalyst. According to (Ramos et al., 2019), the

modification of photocatalyst materials with the addition of sensitizers such as silver or other supporting materials can increase photocatalytic activity. Therefore, the surface area of the ZnO photocatalyst added with graphene will increase alongside pure ZnO. Stengl et al., (2011) also reported that graphene sheets with a large surface area would provide a good effect as a supporting material in the photodegradation process.

Table 1. BET Analysis of Materials

Material	Surface Area (m ² /g)
ZnO*	10.81
ZnO/Graphene-like Composites (700°C)	101.514

*Source: (Rabbani et al., 2021)

UV-Vis DRS (Diffuse Absorbance Spectra) characterization is used to determine the band gap energy of a material. Moreover, band gap energy shows the wavelength of light that is effectively absorbed in the photocatalyst material and is calculated using the following equation (Ahamad & Ahmed, 2023):

$$\alpha = \frac{K}{S} = \frac{1-R^2}{2R} \dots\dots\dots (2)$$

Where: α = Kubelka-Munk factor; K = Absorption coefficient; S = Scattering coefficient; R = Measured reflectance value

Based on the equation, a Tauc plot (E_g versus $(\alpha \cdot hv)^{1/2}$) was constructed, as shown in Figure 5.

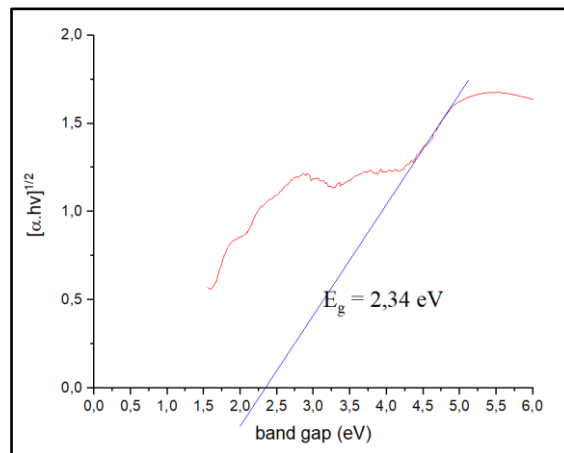


Figure 5. UV-Vis DRS and Tauc plot of ZnO/Graphene-like composites

In Figure 5, the band gap energy of ZnO/graphene-like composites is found to be 2.34 eV. The decrease in band gap energy is originally ZnO (3.37 eV) (Choi et al., 2012) due to the compositing factor with graphene-like based on biochar from oil palm shells. Vinayagam et al. (2018) also reported that non-metallic elements

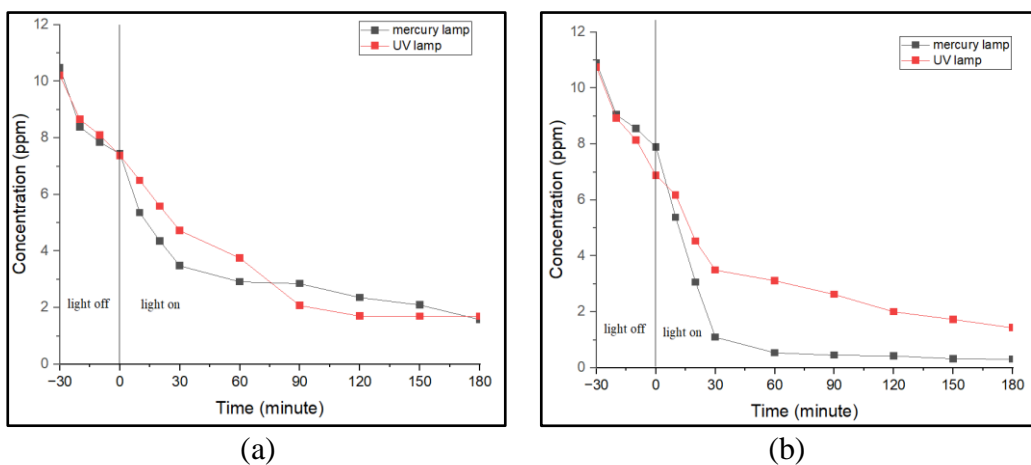
such as C, N, and S successfully reduced the band gap energy of semiconductors with large energy. According to (Mankomal & Kaur, 2022), the lower band gap value in the composite may be due to the porous structure that allows being scattered by light. The reduced band gap energy also causes the light absorption area to be significantly wider, as determined using the formula (Rong et al., 2014):

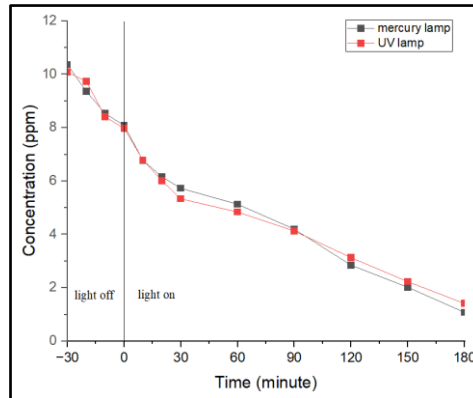
$$E_g = h \times v = h \times \frac{c}{\lambda} \dots\dots\dots (3)$$

Where : E_g = band gap energy (eV), h = Planck constant (6.626×10^{-34} Js), c = speed of light (3×10^8 m/s), λ = wavelength (nm)

Based on the equation and band gap energy value obtained, the wavelength of ZnO/Graphene-like composite is found to be approximately 530 nm. This value was in the visible light region, showing the success of compositing, where the absorption of light was only able in the UV light region. (Zhang et al., 2014) stated that the decrease in ZnO band gap caused by compositing with non-metals such as carbon led to widening the absorption area of ZnO to the visible light region, thereby increasing the photocatalytic process. According to (He et al., 2021), the smaller band gap value and wider absorption area to the visible light region could be due to the formation of Zn-O-C, similar to doping ZnO with carbon.

The results of UV-Vis Spectrophotometer tests are presented in Figure 6, showing a graph of the effect of lamp and photodegradation time on methylene blue, methyl orange, and phenol waste. Methylene blue waste with an initial concentration of 10 ppm was photodegraded by the addition of ZnO/graphene-like composites to UV and mercury lamps for 180 minutes with the initial 30 minutes in light-off conditions. Figure 6(a) shows that the concentration of methylene blue waste decreases with the photodegradation process using both UV and mercury lamps. The results were also obtained during the photodegradation of methyl orange waste, as presented in Figure 6(b), and phenol in Figure 6(c) under the same conditions.

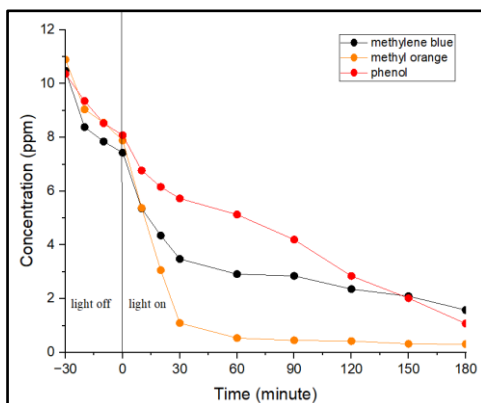




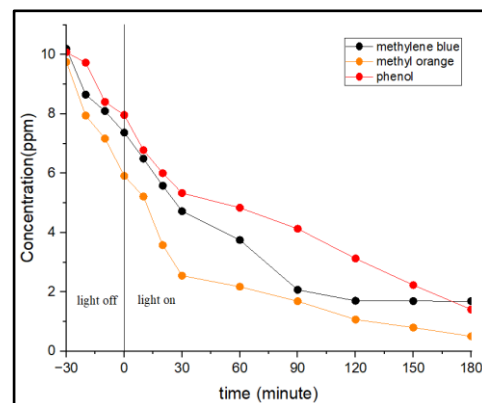
(c)

Figure 6. UV-Vis Spectrophotometer Test (a) Effect of time and light source on methylene blue waste (b) Effect of time and light source on methyl orange waste (c) Effect of time and light source on phenol waste

Figure 7 shows a graph of the effectiveness of lamps on methylene blue, methyl orange, and phenol. In Figure 7(a), the use of mercury lamps was effective against the three wastes with an indication of a constant decrease in concentration. The same results were also obtained when the photodegradation process was carried out using UV lamps, as shown in Figure 7(b).



(a)



(b)

Figure 7. UV-Vis Spectrophotometer Test (a) Effect of mercury lamp on effluent degradation (b) Effect of UV lamp on effluent degradation

Discussion

Figure 6(a) shows the effect of a light source on methylene blue waste with an initial concentration of 10 ppm. The photodegradation process that occurred for 180 minutes with light-off conditions for 30 minutes and light-on for 150 minutes caused a decrease in methylene blue concentration. Percent degradation at 180 minutes for the initial concentration of methylene blue 10 ppm with UV and mercury lamps were 83.42% and 84.93%, respectively, the results of this study are similar to the results of research (Yu et al., 2023) where photodegradation using

ZnO/Graphene-like composites from peanut shells is more effective when illuminated by sunlight whose light intensity is greater and the absorption area is wider than a 350W xenon lamp.

Figure 6(b) shows the effect of a light source on methyl orange waste. Based on the results, the photodegradation process that occurred for 180 minutes with light-off condition for 30 minutes and lights on for 150 minutes caused a decrease in methyl orange concentration. Percent degradation at 180 minutes for the initial concentration of methyl orange with UV and mercury lamps were 94.83% and 97.17%; Respectively, the results of this study are in line with the statement (Peerakiatkhajohn et al., 2021) that the photodegradation of methyl orange using aluminum-doped ZnO under visible light radiation is more effective than irradiation by UV light. This statement is because ZnO experiences an enlargement of the irradiation area to the visible light region due to doping with aluminum.

Figure 6(c) shows that the increasing time of the photodegradation process leads to the degradation of high phenolic compounds. This process was carried out for 180 minutes with the initial 30 minutes of light-off conditions and 150 minutes of light-on. Percent degradation at 180 minutes for the initial concentration of 10 ppm phenol with UV light source and mercury were 86.03% and 89.62%, respectively. It can be seen that the use of mercury lamps appears more effective than UV lamps. (Steiner, 2017) concluded that when the phenol photodegradation process, modified TiO₂ works more effectively in the visible light region than the UV light region because the TiO₂ band gap energy extends to the visible light region.

Based on the results, The intensity of the light source is an important factor in the photodegradation process. (Li et al., 2013) stated that more methylene blue radicals are formed on the surface of the photocatalyst as the intensity of the emitted light increases so that the photodegradation process becomes better. (Groeneveld et al., 2023) argued that higher intensity light results in higher photodegradation efficiency and accelerated reaction rates, as more photons are introduced into the system. However, these statements depend on the capabilities of the composite used and also the waste to be photodegraded. Based on the UV-Vis spectrophotometer results, it can be seen that the use of mercury ray lamps is better in the photodegradation of various types of liquid waste than UV lamps. This is supported by the UV-Vis DRS data in Figure 5 which shows that the ZnO/Graphene-like composite has a band gap value of 2.34 eV which indicates the composite effectively works in the wavelength range of 530 nm which is located in the visible light region (400-800 nm).

Figure 7 shows the effect of using lamps on the effectiveness of the photodegradation process of methylene blue, methyl orange, and phenol. Based on the results, waste with a high percent degradation was obtained from methyl orange waste, which was 97.17% using a mercury lamp. The results are by the research by (Safni et al., 2019), where mercury lamps showed high performance in the use of C-doped TiO₂ catalyst as a photodegradation agent. However, (Yu et al., 2023)

stated that mercury lamps performed better than UV with photodegradation agents in the form of ZnO/Biochar. According to (Groeneveld et al., 2023), the variations in results were caused by different intensities and wavelengths of irradiation.

Conclusion

In conclusion, this research showed that ZnO/graphene-like composites from palm kernel shells were successfully prepared through solvothermal and calcination methods. The results of SEM, XRD, FTIR, and BET characterization showed that the properties of ZnO/Graphene-like composite material were better compared to pure ZnO. UV-Vis DRS characterization showed a reduction in band gap energy of 2.34 eV from the previous 3.37 eV. The performance of ZnO/Graphene-like composites was tested for the degradation of methylene blue, methyl orange, and phenol using UV and mercury lamps, with an initial concentration of 10 ppm. Percent degradation of methylene blue with UV and mercury were 83.42% and 84.93% respectively, while methyl orange with UV and mercury was 94.83% and 97.17%, respectively. Furthermore, the percent degradation of phenol with UV light and mercury was 86.03% and 89.62%, respectively. These results showed that the use of mercury lamps on methyl orange was more effective compared to UV lamps on methylene blue and phenol.

Acknowledgement

The authors are grateful to DIPA LPPM Riau University for providing financial support for this research in the field of science, with contract number: 8221/UN19.5.1.3/A.L.04/2023.

References

- Abnisa, F., Daud, W. M. A. W., Husin, W. N. W., & Sahu, J. N. (2011). Utilization possibilities of palm shell as a source of biomass energy in Malaysia by producing bio-oil in pyrolysis process. *Biomass and Bioenergy*, 35(5), 1863–1872. <https://doi.org/10.1016/j.biombioe.2011.01.033>
- Adeel, M., Saeed, M., Khan, I., Muneer, M., & Akram, N. (2021). Synthesis and Characterization of Co-ZnO and Evaluation of Its Photocatalytic Activity for Photodegradation of Methyl Orange. *ACS Omega*, 6(2), 1426–1435. <https://doi.org/10.1021/acsomega.0c05092>
- Ahamad, T., & Ahmed, A. S. (2023). Influence of graphene oxide on the dielectric properties of biogenically synthesized ZnO nanoparticles. *Hybrid Advances*, 3, 100059. <https://doi.org/10.1016/j.hybadv.2023.100059>
- Ahmad, I., Fasihullah, Q., & Vaid, F. H. M. (2006). Effect of light intensity and wavelengths on photodegradation reactions of riboflavin in aqueous solution. *Journal of Photochemistry and Photobiology B: Biology*, 82(1), 21–27. <https://doi.org/10.1016/j.jphotobiol.2005.08.004>
- Ahmad, R., & Kumar, R. (2010). Adsorption studies of hazardous malachite green

- onto treated ginger waste. *Journal of Environmental Management*, 91(4), 1032–1038. <https://doi.org/10.1016/j.jenvman.2009.12.016>
- Antal, M. J., & Grønli, M. (2003). The art, science, and technology of charcoal production. *Industrial and Engineering Chemistry Research*, 42(8), 1619–1640. <https://doi.org/10.1021/ie0207919>
- Barzinjy, A. A., & Azeez, H. H. (2020). Green synthesis and characterization of zinc oxide nanoparticles using Eucalyptus globulus Labill. leaf extract and zinc nitrate hexahydrate salt. *SN Applied Sciences*, 2(5). <https://doi.org/10.1007/s42452-020-2813-1>
- Behzadi, S., Nonahal, B., Royae, S. J., & Asadi, A. A. (2020). TiO₂/SiO₂/Fe₃O₄ magnetic nanoparticles synthesis and application in methyl orange UV photocatalytic removal. *Water Science and Technology*, 82(11), 2432–2445. <https://doi.org/10.2166/wst.2020.509>
- Bethi, B., Sonawane, S. H., Bhanvase, B. A., & Gumfekar, S. P. (2016). Nanomaterials-based advanced oxidation processes for wastewater treatment: A review. *Chemical Engineering and Processing: Process Intensification*, 109, 178–189. <https://doi.org/10.1016/j.cep.2016.08.016>
- Chen, M., Bao, C., Hu, D., Jin, X., & Huang, Q. (2019). Facile and low-cost fabrication of ZnO/biochar nanocomposites from jute fibers for efficient and stable photodegradation of methylene blue dye. *Journal of Analytical and Applied Pyrolysis*, 139, 319–332. <https://doi.org/10.1016/j.jaap.2019.03.009>
- Chiou, C. H., Wu, C. Y., & Juang, R. S. (2008). Influence of operating parameters on photocatalytic degradation of phenol in UV/TiO₂ process. *Chemical Engineering Journal*, 139(2), 322–329. <https://doi.org/10.1016/j.cej.2007.08.002>
- Choi, K., Kang, T., & Oh, S. G. (2012). Preparation of disk shaped ZnO particles using surfactant and their PL properties. *Materials Letters*, 75, 240–243. <https://doi.org/10.1016/j.matlet.2012.02.031>
- Duan, X., Sun, H., Kang, J., Wang, Y., Indrawirawan, S., & Wang, S. (2015). Insights into Heterogeneous Catalysis of Persulfate Activation on Dimensional-Structured Nanocarbons. *ACS Catalysis*. <https://doi.org/10.1021/acscatal.5b00774>
- Enesca, A., & Isac, L. (2020). The influence of light irradiation on the photocatalytic degradation of organic pollutants. *Materials*, 13(11). <https://doi.org/10.3390/ma13112494>
- Farghali, A. A., Zaki, A. H., & Khedr, M. H. (2016). Control of Selectivity in Heterogeneous Photocatalysis by Tuning TiO₂ Morphology for Water Treatment Applications. *Nanomaterials and Nanotechnology*, 1–6. <https://doi.org/10.5772/62296>
- Groeneveld, I., Kanelli, M., Ariese, F., & van Bommel, M. R. (2023). Parameters that affect the photodegradation of dyes and pigments in solution and on

- substrate – An overview. In *Dyes and Pigments* (Vol. 210). <https://doi.org/10.1016/j.dyepig.2022.110999>
- Hamzah, N., Tokimatsu, K., & Yoshikawa, K. (2019). Solid fuel from oil palm biomass residues and municipal solid waste by hydrothermal treatment for electrical power generation in Malaysia: A review. *Sustainability (Switzerland)*, *11*(4), 1–23. <https://doi.org/10.3390/su11041060>
- He, Y., Wang, Y., Hu, J., Wang, K., Zhai, Y., Chen, Y., Duan, Y., Wang, Y., & Zhang, W. (2021). Photocatalytic property correlated with microstructural evolution of the biochar/ZnO composites. *Journal of Materials Research and Technology*, *11*, 1308–1321. <https://doi.org/10.1016/j.jmrt.2021.01.077>
- Ike, I. A., Karanfil, T., Cho, J., & Hur, J. (2019). Oxidation byproducts from the degradation of dissolved organic matter by advanced oxidation processes – A critical review. *Water Research*, *164*. <https://doi.org/10.1016/j.watres.2019.114929>
- Jarariya, R. (2022). A Review Based on Spinel Ferrite Nanomaterials-MgFe₂O₄-Synthesis of Photocatalytic Dye Degradation in Visible Light Response. *Journal of Environmental Treatment Techniques*, *10*(2), 149–156. <https://dormaj.org/index.php/jett/article/view/535>
- Jin, Z., Xiao, S., Dong, H., Xiao, J., Tian, R., & Chen, J. (2022). Adsorption and catalytic degradation of organic contaminants by biochar : Overlooked role of biochar's particle size. *Journal of Hazardous Materials*, *422*(June 2021), 126928. <https://doi.org/10.1016/j.jhazmat.2021.126928>
- Kang, S., Li, X., Fan, J., & Chang, J. (2012). Characterization of hydrochars produced by hydrothermal carbonization of lignin, cellulose, d-xylose, and wood meal. *Industrial and Engineering Chemistry Research*, *51*(26), 9023–9031. <https://doi.org/10.1021/ie300565d>
- Kant, R. (2012). Textile dyeing industry an environmental hazard. *Natural Science*, *04*(01), 22–26. <https://doi.org/10.4236/ns.2012.41004>
- Kementerian Perindustrian. (2022). *Informasi Industri 2022*. 1–180.
- Kementrian Lingkungan Hidup. (1995). Keputusan Menteri Negara Lingkungan Hidup Nomor 5 Tahun 2014. *Kementrian Lingkungan Hidup*, 49.
- Li, Z., Liu, J., Zhang, F., & Oh, W. (2013). UV and visible light photodegradation effect on Fe – CNT / TiO₂. *36*(2), 293–299.
- Malik, S. N., Ghosh, P. C., Vaidya, A. N., & Mudliar, S. N. (2020). Hybrid ozonation process for industrial wastewater treatment: Principles and applications: A review. *Journal of Water Process Engineering*, *35*(February). <https://doi.org/10.1016/j.jwpe.2020.101193>
- Mankomal, & Kaur, H. (2022). Synergistic effect of biochar impregnated with ZnO nano-flowers for effective removal of organic pollutants from wastewater. *Applied Surface Science Advances*, *12*(October), 100339. <https://doi.org/10.1016/j.apsadv.2022.100339>
- Mecozzi, M., & Sturchio, E. (2017). Computer assisted examination of infrared and

- near infrared spectra to assess structural and molecular changes in biological samples exposed to pollutants: A case of study. *Journal of Imaging*, 3(1). <https://doi.org/10.3390/jimaging3010011>
- Merouani, S., & Hamdaoui, O. (2019). ScienceDirect Sonolytic ozonation for water treatment : efficiency, recent developments, and challenges. *Current Opinion in Green and Sustainable Chemistry*, 18, 98–108. <https://doi.org/10.1016/j.cogsc.2019.03.003>
- Mok, W. S. L., Antal, M. J., Szabo, P., Varhegyi, G., & Zelei, B. (1992). Formation of Charcoal from Biomass in a Sealed Reactor. *Industrial and Engineering Chemistry Research*, 31(4), 1162–1166. <https://doi.org/10.1021/ie00004a027>
- Ong, C. B., Ng, L. Y., & Mohammad, A. W. (2018). A review of ZnO nanoparticles as solar photocatalysts: Synthesis, mechanisms and applications. *Renewable and Sustainable Energy Reviews*, 81(March 2017), 536–551. <https://doi.org/10.1016/j.rser.2017.08.020>
- Parashar, M., & Shukla, V. K. (2020). Synthesis of Zinc Oxide Nanoparticles. *Zinc-Based Nanostructures for Environmental and Agricultural Applications*. <https://doi.org/10.1063/5.0005478>
- Peerakiatkhajohn, P., Butburee, T., Sul, J. H., Thaweesak, S., & Yun, J. H. (2021). Efficient and rapid photocatalytic degradation of methyl orange dye using al/zno nanoparticles. *Nanomaterials*, 11(4), 1–13. <https://doi.org/10.3390/nano11041059>
- Pham, T. D., Bui, T. T., Nguyen, V. T., Van Bui, T. K., Tran, T. T., Phan, Q. C., Pham, T. D., & Hoang, T. H. (2018). Adsorption of polyelectrolyte onto nanosilica synthesized from rice husk: Characteristics, mechanisms, and application for antibiotic removal. *Polymers*, 10(2). <https://doi.org/10.3390/polym10020220>
- Qu, T., Guo, W., Shen, L., Xiao, J., & Zhao, K. (2011). Investigation of biomass torrefaction based on three major components: Hemicellulose, cellulose, and lignin. *Industrial & Engineering Chemistry Research*, 50. <https://doi.org/10.1021/ie1025453>
- Rabbani, M., Shokraiyan, J., Rahimi, R., & Amrollahi, R. (2021). Comparison of photocatalytic activity of ZnO, Ag-ZnO, Cu-ZnO, Ag, Cu-ZnO and TPPS / ZnO for the degradation of methylene blue under UV and visible light irradiation. *Water Science and Technology*, 84(7), 1813–1825. <https://doi.org/10.2166/wst.2021.360>
- Rafiq, A., Ikram, M., Ali, S., Niaz, F., Khan, M., Khan, Q., & Maqbool, M. (2021). Photocatalytic degradation of dyes using semiconductor photocatalysts to clean industrial water pollution. *Journal of Industrial and Engineering Chemistry*, 97, 111–128. <https://doi.org/10.1016/j.jiec.2021.02.017>
- Ramos, P. G., Flores, E., Luyo, C., Sánchez, L. A., & Rodriguez, J. (2019). Fabrication of ZnO-RGO nanorods by electrospinning assisted hydrothermal method with enhanced photocatalytic activity. *Materials Today*

- Communications*, 19(March), 407–412.
<https://doi.org/10.1016/j.mtcomm.2019.03.010>
- Rong, X., Qiu, F., Zhang, C., Fu, L., Wang, Y., & Yang, D. (2014). Preparation, characterization and photocatalytic application of TiO₂ – graphene photocatalyst under visible light irradiation. *Ceramics International*, 1–10. <https://doi.org/10.1016/j.ceramint.2014.10.072>
- Safni, S., Wulanda, V., Khoiriah, K., & Wellia, D. V. (2019). Degradation of Phenol By Photolysis Using N-doped TiO₂ Catalyst. *Jurnal Litbang Industri*, 9, 51–57. <https://doi.org/http://dx.doi.org/10.24960/jli.v8i2.4675.51-57>
- Sayem, M. A., Hossen Suvo, M. A., Syed, I. M., & Bhuiyan, M. A. (2024). Effective adsorption and visible light driven enhanced photocatalytic degradation of rhodamine B using ZnO nanoparticles immobilized on graphene oxide nanosheets. *Results in Physics*, 58(February), 107471. <https://doi.org/10.1016/j.rinp.2024.107471>
- Steiner, M. G. (2017). *Photocatalytic Decomposition of Phenol under Visible and UV Light Utilizing Titanium Dioxide Based Catalysts*. <https://scholars.unh.edu/honors/350>
- Stengl, V., Popelkov, D., & Vl, P. (2011). TiO₂-Graphene Nanocomposite as High Performace Photocatalysts. *Journal of Physical Chemistry*, 115, 25209–25218.
- Sucahya, T. N., Permatasari, N., & Nandiyanto, A. B. D. (2016). Review : Fotokatalis Untuk Pengolahan Limbah Cair. *Jurnal Integrasi Proses*, 6, 1–15.
- Sudhakar, Jaiswal, K. K., Peera, G., & Ramaswamy, A. P. (2017). Green Synthesis of N-Graphene By Hydrothermal-Microwave Irradiation for Alkaline Fuel Cell Application. *International Journal of Recent Scientific Research*, 8(8), 19049–19053.
- Tay-Agbozo, S., Street, S., & Kispert, L. D. (2018). Diffuse-Reflectance Infrared Fourier Transform and Electron Nuclear Double Resonance Study of the Carotenoid Bixin Attached to Irradiated TiO₂. *Journal of Physical Chemistry C*, 122(33), 19075–19081. <https://doi.org/10.1021/acs.jpcc.8b06240>
- Tripathi, M., Sahu, J. N., & Ganesan, P. (2016). Effect of process parameters on production of biochar from biomass waste through pyrolysis: A review. *Renewable and Sustainable Energy Reviews*, 55, 467–481. <https://doi.org/10.1016/j.rser.2015.10.122>
- Tursi, A. (2019). A review on biomass: Importance, chemistry, classification, and conversion. In *Biofuel Research Journal* (Vol. 6, Issue 2, pp. 962–979). Green Wave Publishing of Canada. <https://doi.org/10.18331/BRJ2019.6.2.3>
- Vandevivere, P. C., Bianchi, R., & Verstraete, W. (1998). Review: Treatment and reuse of wastewater from the textile wet-processing industry: review of emerging technologies. *Journal of Chemical Technology & Biotechnology*, 72(4), 289–302. [https://doi.org/10.1002/\(sici\)1097-4660\(199808\)72:4<289::aid-jctb905>3.3.co;2-r](https://doi.org/10.1002/(sici)1097-4660(199808)72:4<289::aid-jctb905>3.3.co;2-r)
- Vinayagam, M., Ramachandran, S., Ramya, V., & Sivasamy, A. (2018).

- Photocatalytic degradation of orange G dye using ZnO/biomass activated carbon nanocomposite. *Journal of Environmental Chemical Engineering*, 6(3), 3726–3734. <https://doi.org/10.1016/j.jece.2017.06.005>
- Wang, J., Quan, X., Chen, S., Yu, H., & Liu, G. (2019). Enhanced catalytic ozonation by highly dispersed CeO₂ on carbon nanotubes for mineralization of organic pollutants. *Journal of Hazardous Materials*, 368(November 2018), 621–629. <https://doi.org/10.1016/j.jhazmat.2019.01.095>
- Weber, K., & Quicker, P. (2018). Properties of biochar. *Fuel*, 217(December 2017), 240–261. <https://doi.org/10.1016/j.fuel.2017.12.054>
- Wijaya, K., Sugiharto, E., Fatimah, I., Sudiono, S., & Kurniaysih, D. (2006). Utilisasi TiO₂-Zeolit dan Sinar UV. *Jurnal Kimia Fisika*, 16(3), 27–36.
- Yi, S., Zou, Y., Sun, S., Dai, F., Si, Y., & Sun, G. (2019). Rechargeable Photoactive Silk-Derived Nanofibrous Membranes for Degradation of Reactive Red 195. *ACS Sustainable Chemistry and Engineering*, 7(1), 986–993. <https://doi.org/10.1021/acssuschemeng.8b04646>
- Yu, S., Zhou, J., Ren, Y., Yang, Z., Zhong, M., Feng, X., Su, B., & Lei, Z. (2023). Excellent adsorptive-photocatalytic performance of zinc oxide and biomass derived N, O-contained biochar nanocomposites for dyes and antibiotic removal. *Chemical Engineering Journal*, 451. <https://doi.org/10.1016/j.cej.2022.138959>
- Zhang, X., Qin, J., Xue, Y., Yu, P., Zhang, B., Wang, L., & Liu, R. (2014). Effect of aspect ratio and surface defects nanorods. *Scientific Reports*, 4–11. <https://doi.org/10.1038/srep04596>